Cell Metabolism
Article

Somatic Progenitor Cell Vulnerability to Mitochondrial DNA Mutagenesis Underlies Progeroid Phenotypes in Polg Mutator Mice

Kati J. Ahlqvist,[1] Riikka H. Hämäläinen,[1] Shuichi Yatsuga,[1] Marko Uutela,[1] Mügen Terzioglu,[6,7] Alexandra Götz,[1] Saara Forsström,[1] Petri Salven,[2] Alexandre Angers-Loustau,[3] Outi H. Kopra,[4,8] Henna Tyynismaa,[1] Nils-Göran Larsson,[6,7] Kirmo Wartiovaara,[3,5] Tomas Prolla,[9] Aleksandra Trifunovic,[6,10] and Anu Suomalainen[1,11,*]

[1]Research Programs Unit, Molecular Neurology, Biomedicum-Helsinki
[2]Research Programs Unit, Molecular Cancer Biology, Biomedicum-Helsinki
[3]Developmental Biology, Institute of Biomedicine
[4]Haartman Institute, Department of Medical Genetics and Research Programs Unit, Molecular Medicine, and Neuroscience Center
[5]Institute of Biotechnology
University of Helsinki, 00290 Helsinki, Finland
[6]Department of Laboratory Medicine, Karolinska Institutet, S-14186 Stockholm, Sweden
[7]Max Planck Institute for Biology of Aging, 50931 Cologne, Germany
[8]Folkhälsan Institute of Genetics, 00290 Helsinki, Finland
[9]University of Wisconsin, Department of Genetics, Madison, WI 53706, USA
[10]Cologne Excellence Cluster on Cellular Stress Responses in Aging-Associated Diseases, Cologne University, D-50674 Cologne, Germany
[11]Helsinki University Central Hospital, Department of Neurology, 00290 Helsinki, Finland
*Correspondence: anu.wartiovaara@helsinki.fi
DOI 10.1016/j.cmet.2011.11.012

SUMMARY

Somatic stem cell (SSC) dysfunction is typical for different progeroid phenotypes in mice with genomic DNA repair defects. MtDNA mutagenesis in mice with defective Polg exonuclease activity also leads to progeroid symptoms, by an unknown mechanism. We found that Polg-Mutator mice had neural (NSC) and hematopoietic progenitor (HPC) dysfunction already from embryogenesis. NSC self-renewal was decreased in vitro, and quiescent NSC amounts were reduced in vivo. HPCs showed abnormal lineage differentiation leading to anemia and lymphopenia. N-acetyl-L-cysteine treatment rescued both NSC and HPC abnormalities, suggesting that subtle ROS/redox changes, induced by mtDNA mutagenesis, modulate SSC function. Our results show that mtDNA mutagenesis affected SSC function early but manifested as respiratory chain deficiency in nondividing tissues in old age. Deletor mice, having mtDNA deletions in postmitotic cells and no progeria, had normal SSCs. We propose that SSC compartment is sensitive to mtDNA mutagenesis, and that mitochondrial dysfunction in SSCs can underlie progeroid manifestations.

INTRODUCTION

Somatic stem cell (SSC) dysfunction has been proposed to lead to decreased ability for tissue regeneration and aging (Schlessinger and Van Zant, 2001; Sharpless and DePinho, 2007). This hypothesis was supported by mouse models with genomic DNA repair defects, which showed premature aging-like phenotypes and severe SSC dysfunction (Frappart et al., 2005; Ito et al., 2004; Narasimhaiah et al., 2005; Nijnik et al., 2007; Rossi et al., 2007). Mice with *Ku70* and *Ku80* inactivation, leading to defective nonhomologous DNA end-joining, had disrupted lymphopoiesis (Gu et al., 1997) as well as decreased amounts of neural and hematopoietic progenitors (Narasimhaiah et al., 2005; Rossi et al., 2007). A mouse model for trichothiodystrophy (TTD), with a nuclear DNA helicase (*xpd*) mutation and defective nucleotide excision repair, showed a premature aging-like phenotype (de Boer et al., 2002), with severe decrease in hematopoietic progenitors (Rossi et al., 2007). Furthermore, mice with ataxia-teleangiectasia (*Atm*) inactivation had reduced cell-cycle checkpoint activity in response to DNA damage and telomeric instability, resulting in infertility and self-renewal defect of hematopoietic stem cells (HSCs) (Barlow et al., 1996; Ito et al., 2004). The progressive bone marrow failure of these mice was associated with elevated reactive oxygen species (ROS), and the HSC defect could be reversed by treating the animals with n-acetyl-L-cysteine (NAC), a compound with antioxidant capacity and an effect on redox balance (Ito et al., 2004). Double inactivation of *Atm* and telomerase RNA component (*Terc*) resulted in a proliferation and self-renewal defect of adult neural stem cells (NSCs) in vitro, as well as decreased amount of dopaminergic neurons in substantia nigra (Wong et al., 2003). These reports indicate that SSCs are sensitive to defects of genomic DNA repair, and suggest a role for ROS and/or redox status in regulating SSC quiescence and proliferation. They also strongly suggest that SSC dysfunction is intimately connected with premature aging-like symptoms in mice.

Increased mitochondrial DNA (mtDNA) mutagenesis can result in progeroid phenotype in mice. "Mutator" mice show extensive mtDNA mutagenesis, with point mutations and complex

rearrangements, because of an inactivated exonuclease function of the mitochondrial replicative DNA polymerase gamma (POLG) (Ameur et al., 2011; Kujoth et al., 2005; Trifunovic et al., 2004; Williams et al., 2010). Their phenotype mimics premature aging, starting from 6–8 months of age, with progressive hair graying, alopecia, osteoporosis, general wasting, and reduced fertility (Kujoth et al., 2005; Trifunovic et al., 2004). Their life span is limited to 13–15 months because of severe anemia, with age-dependent decline in erythro- and lymphopoiesis, recently suggested to be due to HSC dysfunction (Chen et al., 2009; Norddahl et al., 2011). POLG forms the minimal mtDNA replisome together with the mitochondrial single-stranded DNA binding protein and a replicative helicase, Twinkle (Korhonen et al., 2004; Spelbrink et al., 2001). If dominant mutant Twinkle is overexpressed in mice, large-scale mtDNA deletions accumulate in postmitotic tissues (hence the "Deletor" mice), leading to progressive late-onset mitochondrial myopathy at 12 months of age and respiratory chain (RC)-deficient neurons, but normal life span without progeroid features (Tyynismaa et al., 2005).

We asked whether SSC dysfunction could contribute to the mtDNA mutagenesis-linked premature aging, and utilized the two mouse models with mtDNA maintenance defects, Mutator and Deletor, of which only the former showed a premature aging phenotype. We report here NSC and HSC dysfunction in murine mitochondrial progeria.

RESULTS

Old Mutator Neurons and Skeletal Muscle Show Mild Respiratory Chain Deficiency

To characterize the consequences of high mtDNA mutation load in postmitotic cells, we analyzed the activity and presence of RC enzymes of Mutator mice at the time when they already manifest progeroid phenotype, with hair loss, kyphosis, and severe anemia (13–14 months, Figures 1A and 1B). Histochemical enzyme assay of cytochrome *c* oxidase (COX, partially encoded by mtDNA) and succinate dehydrogenase (SDH, nuclear encoded) showed no COX-negative, SDH-positive neurons in the hippocampus or dentate nucleus (Figures 1C and 1D), or any area with large neurons, including the cortex and cerebellum. However, as previously described (Tyynismaa et al., 2005), Deletor mice at the age of 18 months showed occasional COX-negative neurons in all areas harboring large neurons, including hippocampus and dentate nucleus (Figures 1C and 1D). Immunohistochemistry for RC complexes I (Figure 1F and see Figure S1C available online) and II and IV (Figure S1C) showed high content of these complexes, with only occasional CI-low Purkinje cells in cerebellum, and were similar to WT in the cortex even at 46 weeks of age (Figures S1A and S1B). By western blot, Mutator brains showed a tendency to reduced amounts of complex I (80% of WT) and COX (72% of WT) (Figure 1H). No signs of gliosis were seen in the Mutator brain even at the age of 46 weeks, in SVZ, hippocampus, cortex, and striatum (Figures S1F), and the number of neurons was similar in Mutators and WT littermates, when counted from hippocampal regions CA1 and dentate gyrus (Figures S1G and S1H). Skeletal muscle of Mutator showed less than 1% of COX-negative fibers, whereas Deletors showed ~5% of total muscle fibers to be COX negative (Figure 1G), and the heart showed patches of COX-negative cardiomyocytes (data not shown). The late onset of the Mutator mitochondrial myopathy was further supported by the increase of FGF21 cytokine in serum of the Mutators (Figure 1I), which we recently have shown to be secreted from COX-negative muscle fibers in Deletor mice and to correlate with the degree of RC deficiency (Tyynismaa et al., 2010). Contrasting the otherwise good COX activity in CNS, the neurogenic region of subventricular zone (SVZ) (Figures 2A and 2B), and the metabolically active choroid plexus (Figure 1E) had high numbers of COX-negative cells in the Mutators. SVZ was normal in Deletors (Figure 2B), but choroid plexus showed occasional COX-negative cells (Figure 1E). Apoptosis was not induced in the SVZ of 40- to 46-week-old Mutators (Figure S1E).

These results indicate that even at the terminal phase of the severe progeroid phenotype of mtDNA Mutator mice, their neurons and muscle cells can maintain a well-preserved RC.

Mutators Show Decreased Neural Progenitors in the Adult Brains

As the adult Mutator brains showed RC deficiency in SVZ, we asked whether the neural progenitors were affected. We analyzed the presence of quiescent neural progenitors by scoring nestin positivity of adult Mutator brain (Figures 2C and 2D) and compared it to Deletor and WT mice. Statistically significant decrease in nestin-positive cells was seen in >40-week-old Mutator SVZ when compared to WT littermates, whereas Deletors showed WT-like staining. Proliferative CDC47-positive cells in Mutator (Figure 2E) and in Deletor SVZ were similar to WT in all ages. Since the SVZ region is feeding neural progenitors to the olfactory bulb throughout the life, we analyzed the number of olfactory bulb periglomerular cells. The number of calbindin-positive periglomerular cells in Mutator olfactory bulb was similar compared to WT littermates in different time points (Figure 2F). These results show that the amount of nestin-positive NSCs is reduced in the adult Mutator SVZ, but during the restricted lifetime of these mice, this has little effects on olfactory bulb neuronal populations.

Our results show that even at an advanced stage of premature aging syndrome, the central nervous system shows a minimal phenotype, except for partial loss of quiescent nestin-positive SVZ progenitors. Three subtypes of NSCs have been identified from the SVZ region (Miller and Gauthier-Fisher, 2009; Suh et al., 2009). Type B cells, resembling radial glial cells that serve as NSCs during development, are slowly or infrequently dividing, whereas type C cells are actively proliferating. Type B cells express nestin and GFAP, whereas type C cells are both nestin and GFAP negative. Our results strongly suggest that the quiescent type B cells were decreased in the old Mutator brains. However, in Deletors at the age when neurons were clearly affected with RC deficiency (18 months), no indication of abnormal SVZ was seen.

mtDNA Mutagenesis Leads to Decreased Self-Renewal Capacity of Neural Stem Cells In Vitro, Attenuated with NAC Treatment

To obtain understanding of the Mutator SSC phenotype, we cultured NSCs from E11.5–E15.5 Mutator embryos as freely floating neurospheres. Spheres from E15.5 Mutator embryos

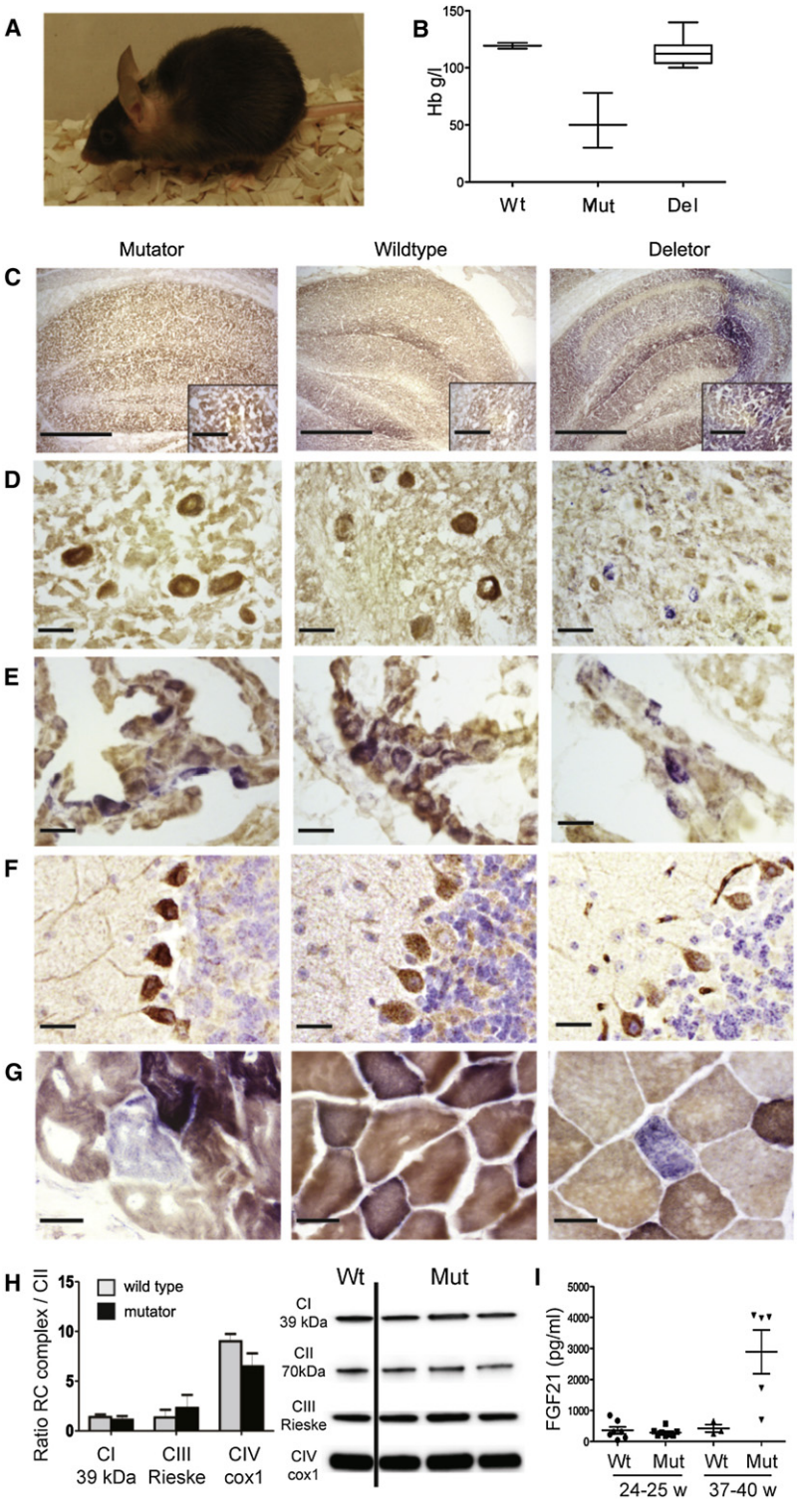

Figure 1. Old Mutator Brain and Skeletal Muscle Show Mild Respiratory Chain Deficiency

(A) At 13 months of age, Mutator mice manifest early-onset progeria with alopecia and kyphosis as well as (B) terminal-stage anemia. Hb values shown as mean ± SD. WT (n = 2), 119.5 ± 3.5; Mutator (n = 3), 52.67 ± 24.1; Deletor (n = 12), 114.1 ± 12.7. (C–G) Samples of Mutator, 13 months; WT, 18 months; Deletor, 18 months. Cryosections showing cytochrome *c* oxidase (COX, brown staining) and succinate dehydrogenase (SDH, blue staining, visible only in cells with COX deficiency) histochemical activity assay from (C) hippocampus (scale bar, 500 μm; insets from CA2 region 10 μm); (D) cerebellar dentate nucleus (scale bar, 20 μm). No COX-negative, SDH^+ cells were found in Mutator hippocampus or cerebellum at the age of terminal manifestation, whereas Deletors at the age of 18 months showed occasional COX-negative, SDH^+ cells (blue) in all areas with large neurons. (E) In metabolically active choroid plexus, Mutators showed high numbers of COX-negative cells (blue), similar to Deletors, but also WT 18-month-old mice had occasional COX-negative cells (scale bars, 10 μm). (F) RC complex I immunohistochemical staining of Purkinje cell layer. Mutators show occasional CI-low cells, but typically excellent staining of CI (brown; counterstained with hematoxylin), whereas Deletors show high variability of CI staining (scale bar, 40 μm). (G) COX-SDH activity assay of frozen sections of skeletal muscle. Less than 1% of Mutator skeletal muscle fibers were COX negative, whereas in Deletors 5% of total muscle fibers were COX negative (scale bar, 20 μm). (H) Mitochondrial extracts from Mutator and WT brain at 39 weeks of age were analyzed by western blot, and Mutator brain showed slightly decreased amount of complexes I (80% of WT) and IV (72% of WT). Complexes I, III, and IV were normalized against nuclear-encoded complex II, and results are shown as mean ±SD. Western blot analysis was done from two separate protein extracts per animal, WT n = 1 and Mutator n = 3. (I) Serum FGF21 concentration is elevated in Mutators only at 37–40 weeks of age (24–25 w; p = 0.559, 37–40 w; p = 0.026). See also Figure S1.

showed significantly higher mtDNA point mutation load compared to the WT spheres (Figure 3A). At the protein level, the increased mtDNA mutations resulted in slight reduction of RC complexes I and IV in NSCs (Figures 3B and 3C), but complexes II and III did not differ from WT when quantified against nuclear-encoded mitochondrial outer membrane protein, porin (Figure 3C). Also the cytochrome *c* oxidase activity was normal (COX activity/mitochondrial matrix enzyme, citrate synthase [CS] activity, WT NSCs [n = 4 lines] 0.66 ± 0.31; Mutator NSCs [n = 3] 0.56 ± 0.06). We next examined whether mtDNA mutations affected the self-renewal capacity of NSCs in vitro. The primary proliferation characteristics of early passage (<6) NSCs, measured by incorporation of BrdU and by flow cytometry, showed that mtDNA mutations did not affect the proliferative activity of NSCs (Figure 3D). To test the NSCs' ability to self-renew, cultures were diluted to clonal density, and the single-cell ability to produce new neurospheres was monitored. Mutator NSCs formed ~3-fold less spheres when compared to WT NSCs (Figure 3E).

We next studied whether the decline in self-renewal ability was affected by increasing redox buffer capacity and antioxidant

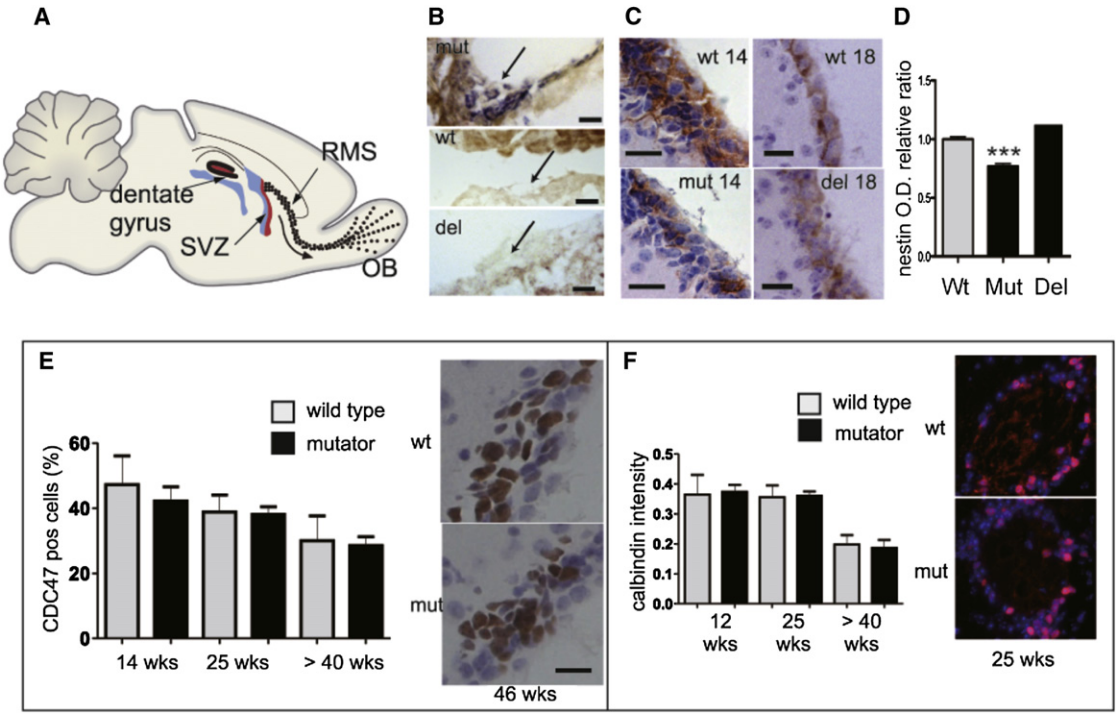

Figure 2. Adult Mutator Brains Show COX-Negative Cells and Decreased Levels of Nestin-Positive NSCs in the SVZ, but the Amount of Proliferative Cells in the SVZ, as well as Olfactory Bulb Interneurons, is Wild-Type Like

(A) Midsagittal view of adult mouse brains showing the areas of neurogenesis in red. Newly formed neural progenitors migrate from SVZ through rostral migratory stream (RMS) to olfactory bulb (OB), where they give rise to interneurons maintaining the OB function.

(B) The SVZ (arrows) had high numbers of COX-negative cells in Mutators, visualized by COX-SDH activity from cryosections (Scale bar, 10 μm), but not in the Deletors or WT mice.

(C) Old Mutator brains at 14 months show decreased number of nestin-positive NSCs in SVZ region, whereas in Deletors at 18 months the NSC numbers did not differ from WT mice.

(D) The relative optical density of the nestin signal was analyzed from SVZ region (600–1,200 cells per sample) and normalized against WT sample. Shown as mean ±SD, ***$p < 0.0001$; animals per genotype, n = 2; scale bar, 20 μm.

(E) Mutators show WT-like amounts of CDC47-positive, proliferating cells in the SVZ area. Five hundred to seven hundred cells per sample were counted, CDC47-positive cells shown as percentage of total cells, mean ±SD. Animals per genotype: 14 weeks, n = 2; 25 weeks, n = 3; >40 weeks, n = 2. Shown is a representative picture of CDC47 immunostaining, proliferating cells seen in brown, from 46-week-old Mutator and WT brains. Scale bar, 20 μm.

(F) The number of olfactory bulb periglomerular interneurons, of which a subset is calbindin positive, was similar to WT in old Mutator brains. Three hundred to four hundred cells per genotype were counted, calbindin-positive cells are shown as percentage of total cells, mean ±SD. Analyzed animals: 12 weeks, n = 1; 25 weeks, n = 2; >40 weeks, n = 2. Shown is a representative picture of calbindin immunostaining from 25-week-old WT and Mutator olfactory bulb (calbindin, red; nuclei, blue).

action. Heterozygous females were fed with NAC throughout the pregnancy and NSCs were extracted from E14.5 embryos, and cultures were supplemented with NAC. Self-renewal ability of treated and nontreated NSCs was monitored and showed that NAC treatment restored the self-renewal ability of Mutator NSCs but had no significant affect on the WT NSCs (Figure 3E). When NAC was administrated only during the in vitro culture, and not during embryonal life, it had no effect on self-renewal ability of any NSCs (data not shown). During long-term culture, Mutator NSCs also showed growth restriction: most lines were unable to grow more than 10 passages, whereas WT neurospheres continued growth unaffected after 50 passages (Figure 3F). NAC treatment was unable to reverse the growth restriction in Mutator NSCs but instead caused high variability to WT NSCs' growth properties (Figure 3G). Next we examined NSCs' multipotency by inducing differentiation of single-cell-derived neurospheres to progenitor lines. Mutator NSCs were able to produce morphologically similar neurons and astrocytes as WT (Figure 3H). Our data show that Mutator NSCs have a WT-like capacity to differentiate to different cell types, but reduced self-renewal capacity, which was attenuated by NAC supplementation. However, the growth defect of long-term cultures was not affected by NAC. These results suggest that the mechanism of NSC self-renewal defect involves ROS/redox status.

Mutators Show Abnormal Fetal Erythropoiesis and Disrupted Hematopoietic Progenitor Differentiation in the Adult Bone Marrow

The Mutator NSC phenotype prompted us to ask whether other stem/progenitor cell compartments were affected in the developing embryo. Adult Mutator mice have been shown to develop severe progressive anemia after 6 months of age (Figure 1B) (Chen et al., 2009; Trifunovic et al., 2004) with progressive dysfunction of bone marrow HSCs (Chen et al., 2009; Norddahl et al., 2011). We could replicate the previous findings from adult bone marrow: despite their severe anemia, the adult Mutator

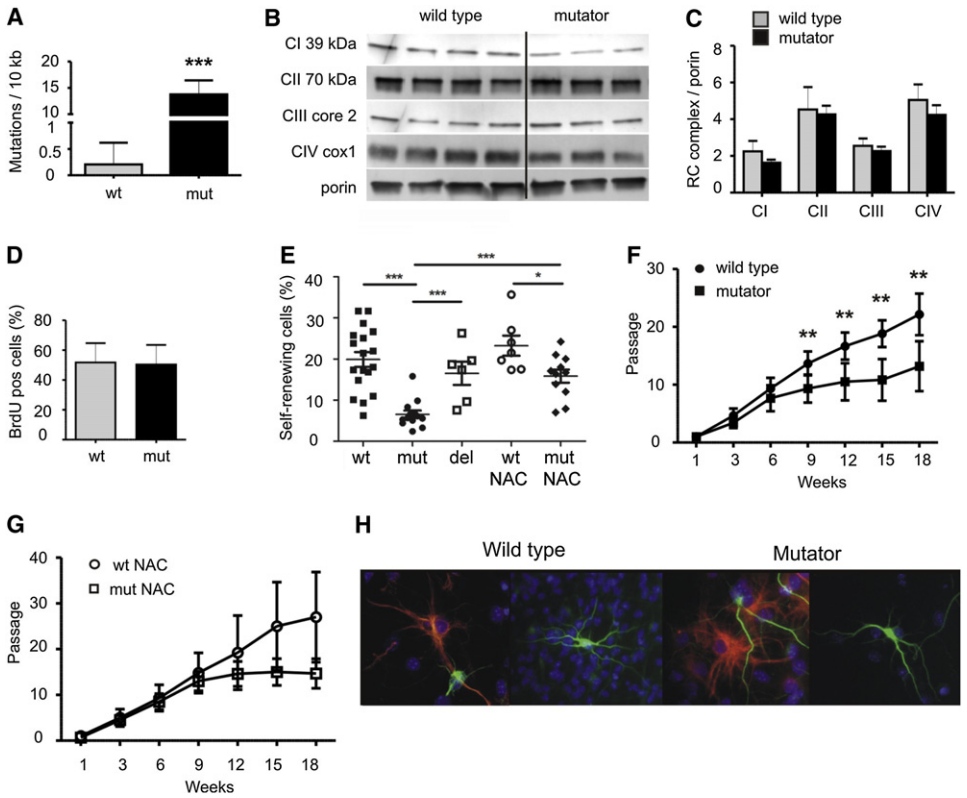

Figure 3. Cultured Mutator NSCs Accumulate mtDNA Point Mutations and Show Decreased Self-Renewal Capacity and Growth Defect in Long-Term Culture, which Can Be Attenuated by NAC Supplementation

(A) Cultured Mutator (n = 3) NSCs from E15.5 embryos showed increase in point mutation load in the cytochrome B gene of mtDNA compared to WT (n = 4) NSCs (Mutator 13.7 mutations/10 kb; WT 0.2 mutations/10 kb).

(B) Mutator NSCs (n = 3) showed slight reduction of RC complexes I and IV analyzed by western blot.

(C) Mutator NSCs (n = 3) RC protein levels were compared to WT NSCs (n = 4), and the amount of RC subunits was normalized to nuclear-encoded mitochondrial porin.

(D) Mutator NSCs (n = 4) showed BrdU incorporation similar to that of WT (n = 8) NSCs, indicating unaffected proliferation capability in flow cytometric analysis when 120,000–240,000 cells per genotype were analyzed. Analysis was performed with low-passage NSCs ($p < 6$).

(E) Mutator NSCs (n = 13) produced significantly less neurospheres than did WT (n = 18; ***$p = < 0.0001$) or Deletor (n = 6; ***$p = 0.0005$) NSCs in clonal expansion analysis, indicating reduced self-renewal capacity. Mutator NSCs with NAC (n = 11) showed improved self-renewal capacity (***$p < 0.0001$), while the treatment had no significant effect on the WT NSCs (n = 7; $p = 0.321$). Altogether 10,500–27,000 cells per genotype were analyzed. Self-renewing cells are shown as a percentage of total cells (mean ±SD): Mutator, 6.5% ± 3.4%, WT, 19.9% ± 7.7%, and Deletor, 16.5% ± 2.8%; Mutator with NAC, 15.8% ± 5.3%, and WT with NAC, 23.3% ± 6.5%.

(F) Mutator NSCs (n = 3) showed growth restriction in continuous long-term culture compared to WT NSCs (n = 5), and the difference between WT and Mutator lines became statistically significant by the ninth week of culture.

(G) The growth restriction of Mutator NSCs was partially attenuated by NAC supplementation: Mutator NSCs with NAC (n = 6) grew slightly better compared to Mutator NSCs but could not reach the same passage levels as WT or WT-NAC (n = 6) lines.

(H) Cultured Mutator NSCs were able to differentiate into both neuronal (Tuj-1, green) and glial (GFAP, red) cells when induced to differentiate with 2% FBS. Hoechst (blue) was used to stain nuclei.

bone marrow showed well-maintained total cellularity (results shown as mean ± SD, WT [n = 2] $9.6 \times 10^6 \pm 1.1 \times 10^6$ and Mutator [n = 2] $7.2 \times 10^6 \pm 2.3 \times 10^6$). Even at 40 weeks, all cell populations expressing the erythroid markers typical for each maturation stage were present, but the erythroid FACS profiles were clearly abnormal, with lower mean intensity of Ter119 signal compared to the WT bone marrow (Figures S2A and S2B). Both the myeloid and B-lymphoid cell numbers were decreased in the 40-week-old adult Mutator bone marrow (Figure S2C).

The end stage severe HSC phenotype suggested that HSCs could be affected already in early phase. We investigated whether the hematopoietic system and erythropoiesis were established during embryonic development. At E13–E15.5, the major site for mouse hematopoiesis is the liver (Ema and Nakauchi, 2000). We detected a decrease in the total amount of cells in Mutator fetal liver extracts compared to WT littermates (Figure 4A). Based on FACS analysis, the major hematopoietic lineages, myeloid and lymphoid, were established normally in Mutator embryos (Figure S2D). However, the relative proportions of different erythroid precursors differed from WT already in the early embryo: basophilic erythroblasts (CD71+,Ter119+ population) progressively decreased in the Mutators (Figure 4B), and the most mature erythroid progenitors (Ter119+,$CD71^{low}$)

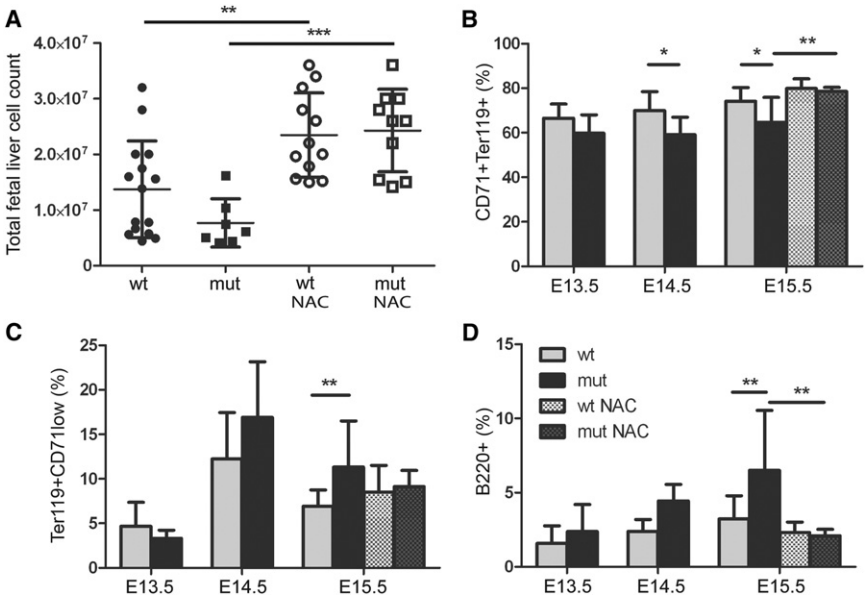

Figure 4. Mutators Show Abnormal Erythropoiesis and Lymphopoiesis Already during Fetal Development, Attenuated by NAC Supplementation

(A) Mutator fetal liver extracts showed slightly decreased amount of total cells compared to WT littermates at E15–E15.5 (WT, n = 15; and Mutator, n = 7; p = 0.099). NAC supplementation during the fetal development increased the total fetal cell count in both WT (n = 12) and Mutator (n = 10) embryos, bringing the Mutator cell number to the same level as the WT. (B) The amount of basophilic erythroblasts (CD71+,Ter119+) progressively decreased during the embryogenesis of Mutator mice, whereas (C) the amount of more mature orthochromatophilic erythroblasts (Ter119+, $CD71^{low}$) increased. NAC supplementation during the fetal development restored both cell populations in Mutator fetal liver to the WT level (E13–E13.5 WT, n = 9; Mutator, n = 8; E14–E14.5 WT, n = 3; Mutator, n = 4; E15.5 WT, n = 15; WT NAC, n = 12; Mutator, n = 7; and Mutator NAC, n = 10). (D) The amount of B220-positive B-lymphoid cells increased in Mutator fetal liver, reaching statistical significance at E15.5 (p = 0.0092), while NAC supplementation during fetal development was able to normalize the frequency of B220-positive cells (E13–E13.5 WT, n = 9; Mutator, n = 5; E14–E14.5 WT, n = 3; Mutator, n = 8; E15.5 WT, n = 15; WT NAC, n = 12; Mutator, n = 7; and Mutator NAC, n = 10). Graphs in (B)–(D) show the percentage of positive cells from total fetal liver cells (mean ±SD).

increased in the fetal liver at E15.5 (Figure 4C). The proerythroblast population (CD71+) was similar to WT (results shown as mean ± SD, E13-E13.5: WT [n = 7] 9.1% ± 2.6% of total cells; Mutator [n = 3] 8.1% ± 0.5%; E15.5: WT [n = 15] 8.4% ± 2.8%; WT NAC [n = 12] 7.5% ± 1.8%, Mutator [n = 7] 8.9% ± 1.5%; Mutator NAC [n = 10] 8.0% ± 0.9%).

We next tested whether we could affect the fetal hematopoietic phenotype with NAC supplementation. Heterozygous females were fed with NAC throughout the pregnancy, and hematopoietic cells were extracted from the liver of E15.5 embryos and subjected to FACS analysis immediately after extraction. The total amount of cells in the fetal liver of Mutators was restored to WT levels by NAC supplementation (Figure 4A). Also the proportions of different erythroid progenitor populations were normalized to WT level in the Mutator embryos treated with NAC (Figures 4B and 4C). We then analyzed the frequency of CD11b-positive myeloid and B220-positive B-lymphoid progenitors in fetal liver and found a progressive increase in the amount of B-lymphoid cells in the Mutators compared to WT littermates (Figure 4D). However, NAC-treated Mutator E15.5 embryos showed B220+ cell amounts similar to those of WT embryos (Figure 4D). These results show that, similar to the NCS defect, the fetal hematopoietic phenotype can be ameliorated by NAC treatment.

To analyze the function of fetal HPCs, we analyzed their ability to produce hematopoietic colonies when plated on methylcellulose. Mutator fetal liver HPCs were able to produce mixed myeloerythroid colonies (CFU-GEMM), whereas erythroid (BFU-E) and granulocyte-macrophage colonies (CFU-GM) were modestly increased in number (Figure S2E). Forty-week-old Mutator bone marrow formed fewer mixed myeloerythroid, erythroid, and granulocyte-macrophage colonies than did WT (Figure S2F). These results show that different lineages of the hematopoietic system appear to be established during embryogenesis, although distorted erythroid and lymphoid lineage differentiation was evident already at the fetal stage. Furthermore, NAC supplementation was able to bring the frequencies of the erythroid and lymphoid cell populations in Mutator fetal liver to WT level.

Deletors Show No mtDNA Deletion Formation in NSCs, and Have Normal NSC Characteristics and Hematopoiesis

Deletor mice, which accumulate mtDNA deletions and have RC deficiency in their postmitotic tissues (Figures 1B–1G) (Tyynismaa et al., 2005), displayed neither increased mtDNA point mutation load (1.1/10 kb in Deletors, 0.7/10 kb in WT littermates) nor mtDNA deletions (data not shown) in their NSCs, and were also able to self-renew (Figure 3E) and differentiate normally when compared to WT littermates. The mutant transgene was expressed in NSCs 2-fold compared to the endogenous gene, which is similar to the level that causes mtDNA deletions in the Deletor skeletal muscle, brain, and heart. Hematopoiesis was normal in the Deletors: their erythroid, lymphoid, and myeloid progenitor amounts were similar to WT both in fetal liver and in adult bone marrow from animals of 110 weeks of age (Figures S2G–S2J). These findings logically show that the mtDNA maintenance defect affects SSC function only when mtDNA mutation load is increased in the stem/progenitor cells themselves.

DISCUSSION

We report here that the mtDNA Mutator mice with premature aging-like syndrome have an embryonal-onset progressive dysfunction of neural and hematopoietic progenitor cells, leading to reduction of quiescent neural progenitors in the SVZ and to severe anemia and lymphopenia in the adults. Previously,

progeroid mice with dysfunctional nuclear DNA repair have been reported to have similar defects. The NSCs of prematurely aging *Atm*$^{-/-}$ *Terc*$^{-/-}$ mice showed reduced self-renewal capacity in vitro and decreased amount of proliferating cells in adult SVZ region in vivo (Wong et al., 2003). *Ku70*$^{-/-}$, *Ku80*$^{-/-}$, and TTD mice showed a decreased amount of hematopoietic progenitors in their bone marrow and defective repopulation activity of HSCs (Gu et al., 1997; Rossi et al., 2007). Similar to Mutators, *Atm*$^{-/-}$ mice showed progressive anemia and decreased amount of granulocyte-macrophage and lymphoid progenitors in their bone marrow (Ito et al., 2004). The close similarities between the stem cell properties of other premature aging models and Mutators emphasize the importance of both nuclear and mtDNA integrity in tissue progenitor homeostasis throughout life.

Parallel to their severe SSC phenotype, the Mutator mice developed modest late-onset signs of mitochondrial RC deficiency in brain, skeletal muscle, and heart. Although an expected consequence in mtDNA Mutator, the surprisingly late and mild nature of RC defect indicates that postmitotic tissues can resist random mtDNA mutagenesis well. We compared the findings in the Mutators to another mouse model with mtDNA maintenance defect, the Deletors. The latter accumulate large-scale mtDNA deletions in postmitotic tissues, leading to late-onset RC deficiency, mimicking the muscle and brain phenotype of Mutators. However, the Deletors have normal SSCs and no premature aging phenotype. These findings support a crucial role of SSC dysfunction in generating the progeroid phenotype of Mutators.

Previously, Mutator brains have been reported to have RC deficiency, based on changes in macroscopic COX-SDH activity, with no data on protein complexes or histology on neuronal level (Ross et al., 2010; Vermulst et al., 2008). We did not find abnormal COX or SDH activities in our old Mutator brains, but only a marginal reduction of complex I and COX protein amounts by western and immunohistochemical analyses. While COX-negative neurons could readily be found in the Deletors, they did not exist in Mutators, suggesting that neurons can compensate random mtDNA mutagenesis well. This is supported by the finding that mice with postnatal disruption of mitochondrial transcription factor A in cortical and hippocampal neurons, leading to loss of mtDNA, survived for months before developing RC dysfunction and neurodegeneration (Sorensen et al., 2001). Based on these results, we propose that the Mutator mice have two separate manifestations: (1) a progeroid syndrome as a consequence of early-onset dysfunction of SSC pool, and (2) a late-onset mild RC deficiency in brain, skeletal muscle, and heart as a consequence of progressive RC dysfunction.

SSC maintenance is dependent on a fine balance of self-renewal and differentiation, in the regulation of which physiological ROS has recently been implicated: low concentrations of ROS, which did not cause detectable DNA, protein, or lipid damage, could shift quiescent SSCs toward proliferation and/or differentiation (Hamanaka and Chandel, 2010; Le Belle et al., 2011; Shao et al., 2011; Yoneyama et al., 2010). Interestingly, the NSC and HPC defects of Mutator could be ameliorated by NAC treatment, suggesting involvement of aberrant ROS signaling or redox status in Mutator somatic precursor cell maintenance. No direct evidence of oxidative damage to proteins, lipids, or nucleic acids was found in the tissues or cells of Mutators (Kujoth et al., 2005; Trifunovic et al., 2005), but their cardiomyopathy was attenuated by overexpression of mitochondrial-targeted catalase, a ROS scavenger (Dai et al., 2010). In *Atm*$^{-/-}$ and *FoxO1/3/4*$^{L/L}$ mice, even a small increase in ROS production in HSCs could affect their quiescence and disrupt their ability to reconstitute their niches (Ito et al., 2004; Tothova et al., 2007). Similar to Mutators, the SSC phenotypes of *Atm*$^{-/-}$ and *FoxO1/3/4*$^{L/L}$ mice could be complemented with NAC. NAC is a thiol, which is readily deacetylated to form L-cysteine, the rate-limiting amino acid for reduced glutathione (GSH) synthesis. Therefore, NAC increases the amount of GSH in cells, improving their redox buffering capacity, but also has direct antioxidant effects (De Flora et al., 1995; Murphy et al., 2011). We suggest that a subtle increase in mitochondrial O_2^- and/or change in the redox status, as a consequence of mtDNA mutagenesis, is sufficient to modify signaling in SSCs and modify their function to severely disrupt SSC homeostasis.

Our data of NSCs and HPCs suggest that the Mutators have a widespread dysfunction of tissue progenitors. The Mutator NSCs showed reduced self-renewal capacity in vitro and failure to maintain proliferation in long-term culture. In adult brains, the number of the quiescent nestin-positive type B neural progenitors of SVZ was decreased, a logical consequence of disability to self-renew. Considering the early-onset NSC defect in vitro in the Mutators, the adult brain phenotype was surprisingly modest, suggesting that the life span of Mutators may be too short to allow full manifestation of late-onset neurodegeneration. No increase of apoptosis in the brain was seen, even in the neurogenic regions, which, however, showed RC deficiency. In Mutator brains, the cells of choroid plexus and SVZ neurogenic area showed high numbers of COX-negative cells. Choroid plexus sometimes shows COX-negative cells even in old WT mice, which is suggested to be caused by high metabolic activity of these cells. However, RC deficiency in potential neural progenitors raises the question of whether these cells preferentially accumulate mtDNA mutations and whether their mtDNA half-life is short and turnover rapid, making them dependent on POLG function. These questions require further attention in the future.

In the adult bone marrow, at the time when the mice suffered from severe anemia, different erythroid progenitor populations were present, but considerable amounts of cells were in intermediate states of maturity, supporting previous results (Chen et al., 2009; Norddahl et al., 2011). Furthermore, we show that Mutator hematopoiesis is affected already during fetal development, when different progenitor populations are all established, but present in aberrant amounts. These data suggest that mtDNA mutagenesis affects the quality of hematopoietic progenitors more than quantity, possibly disturbing their normal quiescent state, which has been suggested to be crucial for reconstitution capacity and long-term sustenance of HSCs (Arai et al., 2004). Although we found no signs of exhaustion of undifferentiated progenitor cells in Mutator bone marrow, our results do suggest deranged differentiation pattern and function of erythroid progenitor populations, which may result in increased apoptosis of hematopoietic cells, as previously suggested (Norddahl et al., 2011), leading to life-threatening anemia. We found mtDNA mutagenesis also to affect lymphopoiesis, leading to lymphopenia in adults, supporting a previous report (Chen et al., 2009).

Paradoxically, Mutator embryos showed increased B-lymphoid cells in the fetal liver, whereas the adult bone marrow showed a low number of B-lymphoid progenitors and decreased ability to produce myeloerythroid colonies. These data further suggest that disrupted proliferation and/or differentiation of the hematopoietic progenitor cells underlies Mutator anemia and lymphopenia.

POLG is part of the minimal replisome of mtDNA together with Twinkle helicase (Korhonen et al., 2004). Because of the necessity of these two proteins for mtDNA replication, their defects could be assumed to affect tissues with high proliferative activity, such as the skin, the gastrointestinal tract, or the blood. However, in humans, recessive POLG and Twinkle mutations result in progressive childhood, juvenile, or adult-onset neurodegenerative disorders, with muscle and brain RC deficiency, but no anemia or lymphopenia, or no apparent signs of premature aging (Suomalainen and Isohanni, 2010). Therefore, it is somewhat surprising that exonuclease deficiency of POLG does not mimic human POLG disorders but affects the proliferative tissues that have high demand for mtDNA replication, especially the progenitor populations. This suggests that catalytic POLG functions involved in mtDNA repair are important for the long-lived brain mtDNAs (Weissman et al., 2007), whereas the proofreading POLG function and faithful mtDNA replication are especially essential in proliferating progenitors. However, no Mutator-like phenotype with extensive random mutagenesis of mtDNA has been characterized in humans, and therefore comparison of Mutator results to human diseases should be done with caution.

Recently, endurance exercise was reported to ameliorate the premature aging symptoms in Mutator mice (Safdar et al., 2011). Exercise has been shown to affect the vitality of muscle and NSCs (Blackmore et al., 2009; Shefer et al., 2010; Wu et al., 2008) and also to promote hematopoiesis (Baker et al., 2011). It remains to be studied whether increased SSC fitness underlies the effect of exercise in Mutators.

We show here that accumulation of mtDNA mutations in Mutator mice already leads to alterations in two distinct stem/progenitor cell compartments during fetal development. RC deficiency in postmitotic tissues is a late phenomenon in these mice, starting to manifest at the time when anemia and lymphopenia are restricting the life of these animals. Our results show that the hematopoietic compartment is especially vulnerable to mtDNA mutagenesis, whereas the nervous system is well preserved. Our results of NAC complementation suggest that the mechanism by which mtDNA mutations affect the homeostasis of tissue progenitors involves physiological ROS/redox signaling in SSCs, repressing quiescence state. Our results strongly suggest that mtDNA mutagenesis in somatic stem/progenitor cells can contribute to aging-related phenotypes.

EXPERIMENTAL PROCEDURES

See also the Supplemental Experimental Procedures.

Mouse Models

All animal experimentation was approved by the Ethical Review Board of Finland. Mice with a knockin inactivating mutation (D257A) in the exonuclease domain of DNA polymerase gamma, PolG (Mutator mice [Kujoth et al., 2005; Trifunovic et al., 2005]), and mice ubiquitously overexpressing mouse Twinkle cDNA with a dominant human disease mutation, leading to duplication of 13 amino acids (dup353–365) in the linker region of mitochondrial Twinkle helicase (Deletor mice [Tyynismaa et al., 2005]), were used. We used two Mutator mouse colonies: one in C57Bl6, originating from T.P., and these mice were used in NSC and HSPC experiments and in western analysis of the RC complexes from NSCs. Embryos for HSPC and NSC extraction, as well as adult brains for immunohistology and histochemistry, were obtained from Mutator colony established by A.T. and N.-G.L.

Analysis of the Respiratory Chain Complexes by Western Blot

Whole-cell protein extraction from NSCs, mitochondrial protein enrichment from brains, SDS-PAGE, and immunodetection of RC complexes were performed as previously described (Ylikallio et al., 2010). For protein detection, we used monoclonal antibodies against the 39 kDa subunit of complex I, core 2 or Rieske subunit of complex III, cox1p subunit of complex IV, 70 kDa Ip subunit of complex II (Mitosciences) and porin (VDAC) (Calbiochem) as a loading control. All samples were analyzed in duplicates.

Respiratory Chain Enzyme Activity Measurements and FGF21

The RC enzyme activity of complex IV (cytochrome *c* oxidase) and the enzyme activity of CS were determined from whole-cell lysates of cultured NSCs as previously described (Suomalainen et al., 1992). All samples were analyzed as duplicates. FGF21 levels in serum of the mice were analyzed by ELISA, with Quantikine mouse FGF-21 Immunoassay kit (R&D Systems, MF2100) as described (Tyynismaa et al., 2010).

NSCs from Embryos

NSCs were extracted from the lateral ventricular wall of E11.5–E15.5 mouse brain as previously described (Piltti et al., 2006). Neurospheres were cultured in serum-free F12 medium (Sigma-Aldrich) supplemented with FGF2 and EGF (Sigma-Aldrich).

mtDNA Deletion and Point Mutation Analysis

DNA from low-passage (<10) neurospheres was extracted by standard phenol-chloroform and ethanol precipitation method. MtDNA deletions were analyzed as previously described (Tyynismaa et al., 2005). For point mutation analysis, the CytB and control region areas of mtDNA were amplified as described (Trifunovic et al., 2004) with a high-fidelity DNA polymerase (Phusion, New England BioLabs). PCR products were cloned into ZeroBlunt Topo vector (Invitrogen) and sequenced. Altogether, 30 kb of sequence was analyzed from each genotype from both CytB and control region using Sequencher software (Genecodes). Single mutations were counted once, to avoid repeated calculations of clonal mutation events, but this strategy ignored same-site mutations.

Analysis of NSC Self-Renewal Capacity

Analysis of NSC self-renewal capacity was performed as previously described (Piltti et al., 2006).

BrdU Incorporation Assay

To determine the proliferation rate, neurospheres were incubated in 10 μM BrdU (BD PharMingen), stained with anti-BrdU and fluorescent secondary antibody, and analyzed using FACSAria Cell Sorter.

N-Acetyl L-Cysteine Supplementation

Mice were given 1 mg/ml of NAC (Sigma-Aldrich) in drinking water throughout the pregnancy. NSCs were extracted from E14.5 embryos, and culture medium for NSCs was supplemented with 100 μM NAC. HSCs were extracted from E15.5 embryos and subjected to FACS analysis immediately after the extraction.

Differentiation Analysis of NSCs

Neurospheres originating from single cells were induced to differentiate using 2% FBS and poly-D-lysine-coated chamber slides; cells were stained with anti-Tuj-1 and anti-GFAP, and presence of neurons and astrocytes was analyzed.

Brain Immunohistochemistry

Brains of Mutator and WT mice aged 12, 14, 25, 40, and 46 weeks and Deletors of 72 weeks were collected and standard hematoxylin and eosin (TissueTek) protocol was used to determine the morphology from paraffin sections. RC complex subunits were visualized using rabbit anti-CI ND-1 (1:500), mouse anti-CI NDUFS3 (1:100), mouse anti-CII 70 kDa subunit (1:200), and mouse anti-CIV II (1:20). Mouse anti-CDC47 (1:200), rabbit anti-cleaved caspase 3 (1:100), mouse anti-nestin (1:200), and mouse anti-myelin basic protein (1:200) were used to visualize proliferating cells, apoptotic cells, neural progenitors, and oligodendrocytes, respectively, together with the biotinylated secondary antibodies from Vector ABC Elite kit (anti-mouse and anti-rabbit, Vector), and developed using DAB Fast Kit (Sigma-Aldrich). Hematoxylin (Tissue Tek) was used as a counterstain. COX-SDH immunohistological analysis was performed as previously described (Tyynismaa et al., 2005). Rabbit anti-GFAP (1:400) and rabbit anti-calbindin (1:200) were used to visualize astrocytes and subset of the periglomerular neurons of the olfactory bulb, respectively, together with Alexa 594 chicken anti-rabbit secondary antibody. Hoechst was used to stain nuclei. IgG from the primary antibody hosts was used as a negative control for the staining. Analysis of optical density (immunoperoxidase staining) or signal intensity (fluorescence staining) was performed using ImageJ software.

Isolation of Hematopoietic Cells from Fetal Liver and Adult Bone Marrow

Embryos were harvested at E13–E15.5, and liver was dissected out and kept on ice in 1% FBS. Fetal liver was mechanically suspended using scissors and 18–25 G needles, and the suspension was filtered through 40 μm filter (Dako) and subjected to cell counting with crystal violet (Sigma-Aldrich). Adult mice were sacrificed; their femoral and tibial bones were cut out and mechanically cleaned. Bone marrow was flushed out with 1 ml of D-MEM supplemented with penicillin-streptomycin and L-glutamine using insuline syringe, filtered through 40 μm filter (Dako), and subjected to cell counting with crystal violet (Sigma-Aldrich). The cells were immediately forwarded to analysis.

Flow Cytometry Analysis of Hematopoietic Tissues

The hematopoietic lineages derived from the fetal livers and adult bone marrows were analyzed using FACSAria Cell Sorter (Beckton Dickinson) and fluorescence-conjugated antibodies against Sca1, CD71, CD11b, CD34, Ter119 (eBioscience), c-kit, and B220. All antibodies except Ter119 were from BD PharMingen, and antibodies were used 1 μg/1 × 10^6 cells for staining. CD16/CD32 blocker (0.25 μg/1 × 10^6 cells) was used to inhibit possible nonspesific binding of the antibodies, and isotype controls (1 μg/1 × 10^6 cells) were used to determine the background fluorescence of the labels. Thirty thousand cells per cell line and antigen set were analyzed.

Hematopoietic Colony-Forming Assay

Presence of clonogenic hematopoietic progenitors in the fetal liver and adult bone marrow was analyzed by culturing HPCs in MethoCult (StemCell Technologies) for myeloerythroid progenitors according to the manufacturer's instructions. Duplicates were made from each sample.

Statistical Analysis

Statistical significance between groups was determined by using Student's t test. Statistical analysis was performed when each group had at least three samples. $p < 0.05$ was considered significant.

SUPPLEMENTAL INFORMATION

Supplemental Information includes two figures and Supplemental Experimental Procedures and can be found with this article online at doi:10.1016/j.cmet.2011.11.012.

ACKNOWLEDGMENTS

We wish to thank the following funding agencies for support: Sigrid Juselius Foundation, Jane and Aatos Erkko Foundation, the Academy of Finland, University of Helsinki, Institute of Molecular Medicine Finland (FIMM), and Biocentrum Helsinki (for A.S.); and Helsinki Biomedical Graduate School (for K.J.A.). We thank Hanna Mikkola for advice and antibodies for HPC FACS experiments and for very helpful discussions about hematopoietic data. The authors are grateful for Anu Harju, Ilse Paetau, Tuula Manninen, Markus Innilä, Minna Teerijoki, Ivana Bratic, Jarmo Palm, Susanna Lauttia, and Katja Piltti for advice and help in experimental procedures. Mika Hukkanen is thanked for help in image analysis.

Received: June 7, 2011
Revised: October 24, 2011
Accepted: November 30, 2011
Published online: January 3, 2012

REFERENCES

Ameur, A., Stewart, J.B., Freyer, C., Hagstrom, E., Ingman, M., Larsson, N.G., and Gyllensten, U. (2011). Ultra-deep sequencing of mouse mitochondrial DNA: mutational patterns and their origins. PLoS Genet. *7*, e1002028. 10.1371/journal.pgen.1002028.

Arai, F., Hirao, A., Ohmura, M., Sato, H., Matsuoka, S., Takubo, K., Ito, K., Koh, G.Y., and Suda, T. (2004). Tie2/angiopoietin-1 signaling regulates hematopoietic stem cell quiescence in the bone marrow niche. Cell *118*, 149–161.

Baker, J.M., De Lisio, M., and Parise, G. (2011). Endurance exercise training promotes medullary hematopoiesis. FASEB J. *25*, 4348–4357.

Barlow, C., Hirotsune, S., Paylor, R., Liyanage, M., Eckhaus, M., Collins, F., Shiloh, Y., Crawley, J.N., Ried, T., Tagle, D., and Wynshaw-Boris, A. (1996). Atm-deficient mice: a paradigm of ataxia telangiectasia. Cell *86*, 159–171.

Blackmore, D.G., Golmohammadi, M.G., Large, B., Waters, M.J., and Rietze, R.L. (2009). Exercise increases neural stem cell number in a growth hormone-dependent manner, augmenting the regenerative response in aged mice. Stem Cells *27*, 2044–2052.

Chen, M.L., Logan, T.D., Hochberg, M.L., Shelat, S.G., Yu, X., Wilding, G.E., Tan, W., Kujoth, G.C., Prolla, T.A., Selak, M.A., et al. (2009). Erythroid dysplasia, megaloblastic anemia, and impaired lymphopoiesis arising from mitochondrial dysfunction. Blood *114*, 4045–4053.

Dai, D.F., Chen, T., Wanagat, J., Laflamme, M., Marcinek, D.J., Emond, M.J., Ngo, C.P., Prolla, T.A., and Rabinovitch, P.S. (2010). Age-dependent cardiomyopathy in mitochondrial mutator mice is attenuated by overexpression of catalase targeted to mitochondria. Aging Cell *9*, 536–544.

de Boer, J., Andressoo, J.O., de Wit, J., Huijmans, J., Beems, R.B., van Steeg, H., Weeda, G., van der Horst, G.T., van Leeuwen, W., Themmen, A.P., et al. (2002). Premature aging in mice deficient in DNA repair and transcription. Science *296*, 1276–1279.

De Flora, S., Cesarone, C.F., Balansky, R.M., Albini, A., D'Agostini, F., Bennicelli, C., Bagnasco, M., Camoirano, A., Scatolini, L., Rovida, A., et al. (1995). Chemopreventive properties and mechanisms of N-acetylcysteine. The experimental background. J. Cell. Biochem. Suppl. *22*, 33–41.

Ema, H., and Nakauchi, H. (2000). Expansion of hematopoietic stem cells in the developing liver of a mouse embryo. Blood *95*, 2284–2288.

Frappart, P.O., Tong, W.M., Demuth, I., Radovanovic, I., Herceg, Z., Aguzzi, A., Digweed, M., and Wang, Z.Q. (2005). An essential function for NBS1 in the prevention of ataxia and cerebellar defects. Nat. Med. *11*, 538–544.

Gu, Y., Seidl, K.J., Rathbun, G.A., Zhu, C., Manis, J.P., van der Stoep, N., Davidson, L., Cheng, H.L., Sekiguchi, J.M., Frank, K., et al. (1997). Growth retardation and leaky SCID phenotype of Ku70-deficient mice. Immunity *7*, 653–665.

Hamanaka, R.B., and Chandel, N.S. (2010). Mitochondrial reactive oxygen species regulate cellular signaling and dictate biological outcomes. Trends Biochem. Sci. *35*, 505–513.

Ito, K., Hirao, A., Arai, F., Matsuoka, S., Takubo, K., Hamaguchi, I., Nomiyama, K., Hosokawa, K., Sakurada, K., Nakagata, N., et al. (2004). Regulation of oxidative stress by ATM is required for self-renewal of haematopoietic stem cells. Nature *431*, 997–1002.

Korhonen, J.A., Pham, X.H., Pellegrini, M., and Falkenberg, M. (2004). Reconstitution of a minimal mtDNA replisome in vitro. EMBO J. *23*, 2423–2429.

Kujoth, G.C., Hiona, A., Pugh, T.D., Someya, S., Panzer, K., Wohlgemuth, S.E., Hofer, T., Seo, A.Y., Sullivan, R., Jobling, W.A., et al. (2005). Mitochondrial DNA mutations, oxidative stress, and apoptosis in mammalian aging. Science *309*, 481–484.

Le Belle, J.E., Orozco, N.M., Paucar, A.A., Saxe, J.P., Mottahedeh, J., Pyle, A.D., Wu, H., and Kornblum, H.I. (2011). Proliferative neural stem cells have high endogenous ROS levels that regulate self-renewal and neurogenesis in a PI3K/Akt-dependant manner. Cell Stem Cell *8*, 59–71.

Miller, F.D., and Gauthier-Fisher, A. (2009). Home at last: neural stem cell niches defined. Cell Stem Cell *4*, 507–510.

Murphy, M.P., Holmgren, A., Larsson, N.G., Halliwell, B., Chang, C.J., Kalyanaraman, B., Rhee, S.G., Thornalley, P.J., Partridge, L., Gems, D., et al. (2011). Unraveling the biological roles of reactive oxygen species. Cell Metab. *13*, 361–366.

Narasimhaiah, R., Tuchman, A., Lin, S.L., and Naegele, J.R. (2005). Oxidative damage and defective DNA repair is linked to apoptosis of migrating neurons and progenitors during cerebral cortex development in Ku70-deficient mice. Cereb. Cortex *15*, 696–707.

Nijnik, A., Woodbine, L., Marchetti, C., Dawson, S., Lambe, T., Liu, C., Rodrigues, N.P., Crockford, T.L., Cabuy, E., Vindigni, A., et al. (2007). DNA repair is limiting for haematopoietic stem cells during ageing. Nature *447*, 686–690.

Norddahl, G.L., Pronk, C.J., Wahlestedt, M., Sten, G., Nygren, J.M., Ugale, A., Sigvardsson, M., and Bryder, D. (2011). Accumulating mitochondrial DNA mutations drive premature hematopoietic aging phenotypes distinct from physiological stem cell aging. Cell Stem Cell *8*, 499–510.

Piltti, K., Kerosuo, L., Hakanen, J., Eriksson, M., Angers-Loustau, A., Leppa, S., Salminen, M., Sariola, H., and Wartiovaara, K. (2006). E6/E7 oncogenes increase and tumor suppressors decrease the proportion of self-renewing neural progenitor cells. Oncogene *25*, 4880–4889.

Ross, J.M., Oberg, J., Brene, S., Coppotelli, G., Terzioglu, M., Pernold, K., Goiny, M., Sitnikov, R., Kehr, J., Trifunovic, A., et al. (2010). High brain lactate is a hallmark of aging and caused by a shift in the lactate dehydrogenase A/B ratio. Proc. Natl. Acad. Sci. USA *107*, 20087–20092.

Rossi, D.J., Bryder, D., Seita, J., Nussenzweig, A., Hoeijmakers, J., and Weissman, I.L. (2007). Deficiencies in DNA damage repair limit the function of haematopoietic stem cells with age. Nature *447*, 725–729.

Safdar, A., Bourgeois, J.M., Ogborn, D.I., Little, J.P., Hettinga, B.P., Akhtar, M., Thompson, J.E., Melov, S., Mocellin, N.J., Kujoth, G.C., et al. (2011). Endurance exercise rescues progeroid aging and induces systemic mitochondrial rejuvenation in mtDNA mutator mice. Proc. Natl. Acad. Sci. USA *108*, 4135–4140.

Schlessinger, D., and Van Zant, G. (2001). Does functional depletion of stem cells drive aging? Mech. Ageing Dev. *122*, 1537–1553.

Shao, L., Li, H., Pazhanisamy, S.K., Meng, A., Wang, Y., and Zhou, D. (2011). Reactive oxygen species and hematopoietic stem cell senescence. Int. J. Hematol. *94*, 24–32.

Sharpless, N.E., and DePinho, R.A. (2007). How stem cells age and why this makes us grow old. Nat. Rev. Mol. Cell Biol. *8*, 703–713.

Shefer, G., Rauner, G., Yablonka-Reuveni, Z., and Benayahu, D. (2010). Reduced satellite cell numbers and myogenic capacity in aging can be alleviated by endurance exercise. PLoS ONE *5*, e13307. 10.1371/journal.pone.0013307.

Sorensen, L., Ekstrand, M., Silva, J.P., Lindqvist, E., Xu, B., Rustin, P., Olson, L., and Larsson, N.G. (2001). Late-onset corticohippocampal neurodepletion attributable to catastrophic failure of oxidative phosphorylation in MILON mice. J. Neurosci. *21*, 8082–8090.

Spelbrink, J.N., Li, F.Y., Tiranti, V., Nikali, K., Yuan, Q.P., Tariq, M., Wanrooij, S., Garrido, N., Comi, G., Morandi, L., et al. (2001). Human mitochondrial DNA deletions associated with mutations in the gene encoding Twinkle, a phage T7 gene 4-like protein localized in mitochondria. Nat. Genet. *28*, 223–231.

Suh, H., Deng, W., and Gage, F.H. (2009). Signaling in adult neurogenesis. Annu. Rev. Cell Dev. Biol. *25*, 253–275.

Suomalainen, A., and Isohanni, P. (2010). Mitochondrial DNA depletion syndromes—many genes, common mechanisms. Neuromuscul. Disord. *20*, 429–437.

Suomalainen, A., Majander, A., Haltia, M., Somer, H., Lonnqvist, J., Savontaus, M.L., and Peltonen, L. (1992). Multiple deletions of mitochondrial DNA in several tissues of a patient with severe retarded depression and familial progressive external ophthalmoplegia. J. Clin. Invest. *90*, 61–66.

Tothova, Z., Kollipara, R., Huntly, B.J., Lee, B.H., Castrillon, D.H., Cullen, D.E., McDowell, E.P., Lazo-Kallanian, S., Williams, I.R., Sears, C., et al. (2007). FoxOs are critical mediators of hematopoietic stem cell resistance to physiologic oxidative stress. Cell *128*, 325–339.

Trifunovic, A., Wredenberg, A., Falkenberg, M., Spelbrink, J.N., Rovio, A.T., Bruder, C.E., Bohlooly, Y.M., Gidlof, S., Oldfors, A., Wibom, R., et al. (2004). Premature ageing in mice expressing defective mitochondrial DNA polymerase. Nature *429*, 417–423.

Trifunovic, A., Hansson, A., Wredenberg, A., Rovio, A.T., Dufour, E., Khvorostov, I., Spelbrink, J.N., Wibom, R., Jacobs, H.T., and Larsson, N.G. (2005). Somatic mtDNA mutations cause aging phenotypes without affecting reactive oxygen species production. Proc. Natl. Acad. Sci. USA *102*, 17993–17998.

Tyynismaa, H., Mjosund, K.P., Wanrooij, S., Lappalainen, I., Ylikallio, E., Jalanko, A., Spelbrink, J.N., Paetau, A., and Suomalainen, A. (2005). Mutant mitochondrial helicase Twinkle causes multiple mtDNA deletions and a late-onset mitochondrial disease in mice. Proc. Natl. Acad. Sci. USA *102*, 17687–17692.

Tyynismaa, H., Carroll, C.J., Raimundo, N., Ahola-Erkkila, S., Wenz, T., Ruhanen, H., Guse, K., Hemminki, A., Peltola-Mjosund, K.E., Tulkki, V., et al. (2010). Mitochondrial myopathy induces a starvation-like response. Hum. Mol. Genet. *19*, 3948–3958.

Vermulst, M., Wanagat, J., Kujoth, G.C., Bielas, J.H., Rabinovitch, P.S., Prolla, T.A., and Loeb, L.A. (2008). DNA deletions and clonal mutations drive premature aging in mitochondrial mutator mice. Nat. Genet. *40*, 392–394.

Weissman, L., de Souza-Pinto, N.C., Stevnsner, T., and Bohr, V.A. (2007). DNA repair, mitochondria, and neurodegeneration. Neuroscience *145*, 1318–1329.

Williams, S.L., Huang, J., Edwards, Y.J., Ulloa, R.H., Dillon, L.M., Prolla, T.A., Vance, J.M., Moraes, C.T., and Zuchner, S. (2010). The mtDNA mutation spectrum of the progeroid Polg mutator mouse includes abundant control region multimers. Cell Metab. *12*, 675–682.

Wong, K.K., Maser, R.S., Bachoo, R.M., Menon, J., Carrasco, D.R., Gu, Y., Alt, F.W., and DePinho, R.A. (2003). Telomere dysfunction and Atm deficiency compromises organ homeostasis and accelerates ageing. Nature *421*, 643–648.

Wu, C.W., Chang, Y.T., Yu, L., Chen, H.I., Jen, C.J., Wu, S.Y., Lo, C.P., and Kuo, Y.M. (2008). Exercise enhances the proliferation of neural stem cells and neurite growth and survival of neuronal progenitor cells in dentate gyrus of middle-aged mice. J. Appl. Physiol. *105*, 1585–1594.

Ylikallio, E., Tyynismaa, H., Tsutsui, H., Ide, T., and Suomalainen, A. (2010). High mitochondrial DNA copy number has detrimental effects in mice. Hum. Mol. Genet. *19*, 2695–2705.

Yoneyama, M., Kawada, K., Gotoh, Y., Shiba, T., and Ogita, K. (2010). Endogenous reactive oxygen species are essential for proliferation of neural stem/progenitor cells. Neurochem. Int. *56*, 740–746.